Astronomy
&
Astrophysics

First observations of the X-ray transient EXO 2030+375 with IBIS/ISGRI[*]

S. Kuznetsov[1], M. Falanga[1], P. Blay[2], A. Goldwurm[1], P. Goldoni[1], and V. Reglero[2]

[1] CEA Saclay, DSM/DAPNIA/Service d'Astrophysique, 91191 Gif-sur-Yvette Cedex, France
[2] GACE, Instituto de Ciencia de los Materiales, Universitat de Valencia, PO Box 22085, 46071 Valencia, Spain

Abstract. We present a first INTEGRAL observation of the 42 s transient X-ray pulsar EXO 2030+375 with IBIS/ISGRI. The source was detected during Cyg X-1 observations in December 2002. We analyzed observations during the outburst period from 9 to 21 December 2002 with a total exposure time of ~770 kilosec. EXO 2030+375 was almost always detected during single ~30 min exposures in the 18−45 energy bands. The source light curve shows the characteristic outburst shape observed in this source.

Key words. gamma rays: observations – X-rays: individual: EXO 2030+375 – telescopes: INTEGRAL: IBIS

1. Introduction

EXO 2030+375 is a member of the Be/X-ray transients systems, which are the most common type of accreting X-ray pulsar. They consist of an accreting neutron star and a *B* spectral main-sequence donor star that shows Balmer emission lines (Apparao 1994 for review). The line emission is believed to be associated with an equatorial outflow of material expelled from the rapidly rotating Be star that forms a quasi-Keplerian disk near the Be star (Quirrenbach et al. 1997). The X-ray emission of the transient pulsar EXO 2030+375 is modulated by ≈42 s pulsations and periodic ≈46 days type I outbursts, that are produced at each periastron passage of the neutron star, i.e. when the pulsar interacts with the disk of the Be star.

EXO 2030+375 was discovered in 1985 May with EXOSAT satellite during a large outburst phase (Parmar et al. 1989b). This outburst was first detected at a 1−20 keV energy band and its luminosity is close to the Eddington limit (assuming 5 kpc distance to the source) for a neutron star (Parmar et al. 1985). During the later EXOSAT observations a monotonic decline in intensity was seen over nearly 3 orders of magnitude. During this luminosity decline, the intrinsic spin period changed dramatically, with a characteristic spin-up timescale $-P/\dot{P} \approx 30$ years (Parmar et al. 1989b), the energy spectrum (Reynolds et al. 1993), and the 1−10 keV pulse profile (Parmar et al. 1989a) all showed significant

luminosity dependence. Such a spin-up indicates the presence of an accretion disk penetrating well inside the corotation radius. Further evidence of an accretion disk resulted from the detection of 0.2 Hz quasi-periodic oscillations (Angelini et al. 1989).

The shape of the continuum X-ray spectrum in the range 2−25 keV of EXO 2030+375 can be represented by a power-law ($\alpha \approx 1.5$) modified at energies above a high energy cutoff $E_{\mathrm{cut}} \approx 20$ keV with $E_{\mathrm{fold}} \approx 30$ keV (Reynolds et al. 1993). Evidence of a possible cyclotron feature at 36 keV was found in spectra with RXTE observations (Reig & Coe 1999).

We report first observation results of EXO 2030+375 made with INTEGRAL/ISGRI during the Performance and Verification (PV) phase. The source was observed for more than 10 days in different offaxis position.

2. Instruments and observations

The International Gamma-Ray Astrophysics Laboratory (INTEGRAL) (Winkler et al. 2003) is a 15 keV–10 MeV gamma-ray observatory with concurrent source monitoring at X-rays (3−35 keV) and in the optical range (*V*, 500−600 nm). The INTEGRAL main gamma-ray instruments are the spectrometer SPI and the imager IBIS, the supplementary instruments are the X-ray monitor JEM-X and the Optical Monitoring Camera OMC. This provide a combination of imaging and spectropy over a wide range of X-ray and gamma-ray energies including optical monitoring.

The imager IBIS with a angular resolution of 12′ FWHM, a wide full coded field of view (FOV) of 9° × 9° and a partially coded FOV of 29° × 29° (Ubertini et al. 2003) consists of two detection layers, ISGRI and PICsIT.

The front layer ISGRI (Lebrun et al. 2003) is sensitive for lower energy (15 keV−1 MeV), and while its peak sensitivity is between 15 keV and 200 keV, the second one PICsIT (Di Cocco et al. 2003) is sensitive between ∼200 keV and ∼8 MeV. The division into two layers allowed the paths of the photons to be tracked in 3D, as they scatter and interact with more than one element. This offers the possibility to operate IBIS in the additional "Compton mode". The present results of the analyzed data are produced by the ISGRI detector layer.

The Cygnus region, including in the field of view Cyg X-1 (Laurent et al. 2003), Cyg X-3 (Goldoni et al. 2003) and EXO 2030+375 was observed 15 November−21 December 2002. The main target, observed in different position, was Cyg X-1 (Bazzano et al. 2003). During this period EXO 2030+375 was in the IBIS/ISGRI field of view and detected in the outbursts, i.e., in the periastron passage phase starting from December 9th, 2002. In this Letter we report on results of analysis of EXO 2030+375 observations carried out by IBIS/ISGRI in 9−21 December 2002.

3. Data reduction

During the PV phase of observations, the instrument parameters and moreover the pointing direction frequently changed and EXO 2030+375 was not fully coded during all analysed observations. We used observational data starting from December 9th, 2002 when source appeared in the X-ray image of Cygnus region and was reliably detected by IBIS/ISGRI. We rejected observations carried out in slew mode and those in which PICsIT was operated in "Photon-by-Photon" mode.

For light curve data we analyzed observations starting with the outburst phase of EXO 2030+375 from 9 December and lasting to 21 December 2002. These observations correspond to INTEGRAL orbit revolutions 19−22. Table 1 summarizes the observations time and mean source flux for each revolution.

The images produced by the telescope were analysed using the ISDC public software and software developed at our institute for calibration (INTEGRAL Off-line Scientific Analysis (OSA) v1.1 with latest versions of ii_skyimage 3.5 and ii_spectra_extract 1.9). The images were deconvolved using the procedures described in Goldwurm et al. (2003) to recover source position and flux.

4. Imaging and light curve

Cyg X-1 is one of the brightest hard X-ray sources in the sky. It was the main target of the IBIS/ISGRI pointing observations in December 2002 of the Cygnus region. EXO 2030+375 and Cyg X-3 are two other X-ray sources in the vicinity of Cyg X-1 (see Fig. 1). All three sources were in the IBIS/ISGRI field of view during monitoring of this part of X-ray sky. The effective coded area of source on the detector plane decreased consequently from ∼80%−100% in revolution 19 to ∼50%−80% in revolution 22.

Before the image reconstruction and the extraction of light curve from the data we studied the source intensity in different energy bands. Spectral shape of EXO 2030+375 is well approximated by a power-law spectrum with a high energy cutoff
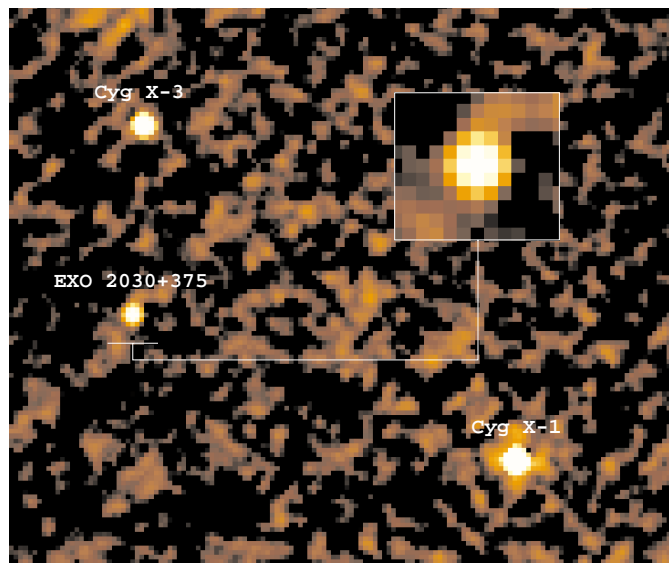

Fig. 1. Image of Cygnus region in 18–45 keV energy band averaged over 142 ksec of observations during 19th revolution. Image size is ∼9°.7 × 11°.7, size of zoomed region of EXO 2030+375 centered at $20^h32^m19^s.8 + 37°38^m15^s.5$ is 0°.9 × 0°.9. Sources were detected with following significance of 1300σ, 210σ and 90σ for Cyg X-1, Cyg X-3 and EXO 2030+375, respectively. Squared root scale was used for color representation.

Table 1. Observation log and average fluxes of EXO 2030+375 in the period of 9−21 December 2002.

Revolution number	Start − Stop time, MJD	Total exp., ksec	Eff. exp., ksec	18−45 keV flux, cnt/s
19	52617.3−52620.1	192	142	5.42 ± 0.05
20	52620.4−52623.0	179	56	7.82 ± 0.08
21	52623.3−52626.1	185	111	6.50 ± 0.07
22	52626.3−52629.0	214	165	2.63 ± 0.07

(Reynolds et al. 1993). Therefore we preferred to select softer energy channels than harder ones in order to avoid possible contamination of the source flux by background radiation. For revolutions 19−22 the level of background radiation is not well established or at least not as well as for later observations when parameters of "veto" were fixed. We found that both observational parameters of EXO 2030+375 – count rate and significance of the detection level of source flux have maximum in 18−45 keV energy range. We used this energy band over our analysis.

The image of the Cygnus region in 18−45 keV energy range averaged over all "Science Window" observations carried out in the course of the revolution 19 is shown in Fig. 1. We detected Cyg X-1 with unprecedented significance of ∼1300σ level. Its X-ray flux dominated over Cyg X-3 and EXO 2030+375 fluxes which were detected with significance levels ∼10−20 times lower (see Fig. 1) than Cyg X-1.

In order to get EXO 2030+375 light curve in 18−45 keV we extracted source count rate from deconvolved image of every "Science Window" observation. The image analysis pipeline
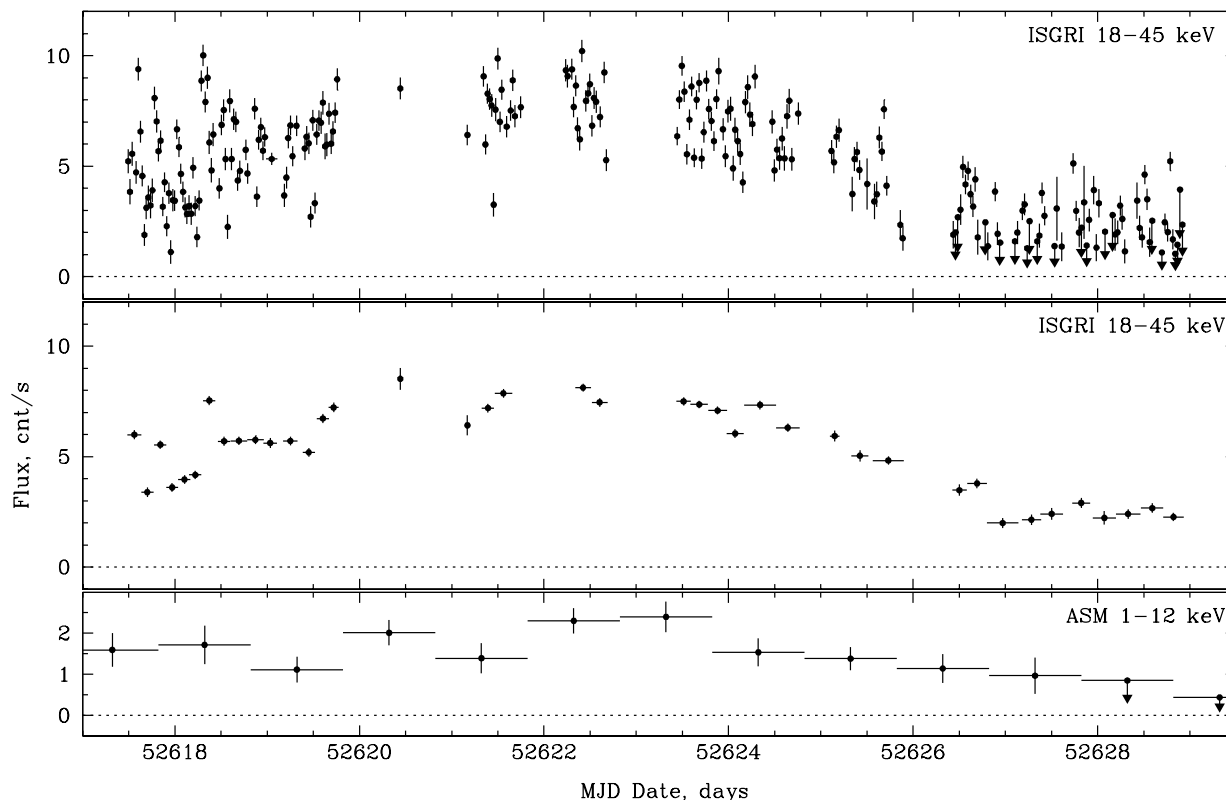
Fig. 2. Light curves of EXO 2030+375 in 18−45 keV (top and middle) and 1−12 keV energy bands. Data points of top pannel correspond to observations of each particular "Science Window" and count rate was extracted directly from source reconstructed spectra. Source flux below 2σ detection level replaced by 2σ upper limits. Data averaged over 1−6 "Science Windows" are shown in middle panel. Light curve obtained bt RXTE All Sky Monitor (ASM) is shown in bottom for comparison. Correlation of source fluxes between in IBIS/ISGRI and RXTE/ASM observations is apparent.

allows to get and estimate intensity of interesting sources directly in output of files. Unfortunately EXO 2030+375 flux extracted in a such way was found at too low intensity level in some part of observational data. In order to check the flux determination procedure we extracted source count rate directly from source reconstructed spectra and compared results of both methods. It was found that extraction of count rate from source spectrum is a more reliable and stable method than the extraction from images. The problem was due to the fact that the detector's count rate is dominated by very strong hard X-ray source like Cyg X-1.

Light curve of EXO 2030+375 is shown in Fig. 2. In order to compare IBIS/ISGRI results with results obtained with other observatories we plotted RXTE/ASM data in the bottom of Fig. 2. The correlation between averaged 18−45 keV IBIS/ISGRI flux and 1−12 keV flux of RXTE/ASM is apparent. The maximum intensity of outburst of ∼8−10 cnt/s ocurred during MJD ∼52 620−52 624. This outburst was also detected by JEM-X (Martinez et al. 2003).

The time range of the first and the last observed photon event correspond to the orbital phase of EXO 2030+375 from 0.9849 to 0.2332. The periastron passage was at the orbital phase zero at 2 452 618.683 JD ∼ 2.8 days before the outburst maximum, according to the epemeries given by Wilson et al. (2002).

5. Spectral analysis

Only fully coded observations of EXO 2030+375 were used to analyze spectral shape. Due to some uncertainties in calculations of counts in spectral bins in partially coded observations, such data were not used for averaged spectrum (nevertheless we used them for light curve shown in Fig. 2). Due to absence of fully coded observations of EXO 2030+375 in revolutions 20−22 spectral analysis was not performed using these revolutions.

Spectral extraction was performed for each particular "Science Window". Source spectra of 31 "Science Window" of fully coded observations of EXO 2030+375 with total integration time of ∼49 ksec were averaged in 13 channels rebinned from 2048 channels of the original matrix. We fitted the intensities of the background and the 3 IBIS/ISGRI sources (Cyg X-1, Cyg X-3 and EXO 2030+375) in the field of view for each spectral bin. The averaged spectrum of EXO 2030+375 is shown in Fig. 3.

We used the 22−100 kev energy range for spectral fit. Power-law model with exponential cutoff was used to approximate the spectral data. It can be seen from the Fig. 3 that the 2nd spectral bin corresponding to the ∼25−30 keV energy band deviates from the expected spectral shape. This bin was excluded from spectral analysis as the observed feature is due to a known problem in the present correction tables used to
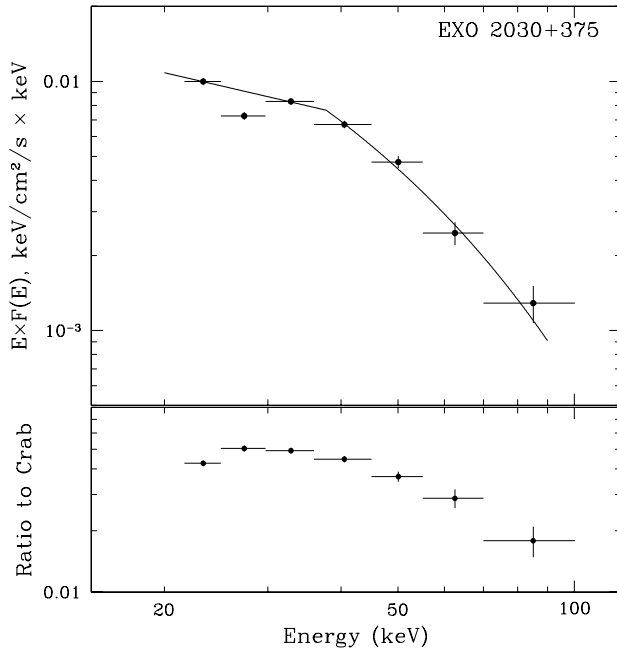
Fig. 3. E-folded spectrum of EXO 2030+375 in 20−100 keV energy range averaged over 31 science windows of revolution 19. Only images for which the source was fully coded were used for sum. Total accumulated time is ~49 ksec. Spectral fit by power-law model with high energy cutoff is shown by the solid line. Ratio to e-folded spectrum of Crab is shown for comparison in the bottom.

convert event amplitude channels in deposited energies. In order to demonstrate it we present the ratio of the EXO 2030+357 spectrum to the Crab one in the bottom of Fig. 3. As it can be seen from Fig. 3, the spectral shape of EXO 2030+375 is relatively smooth in comparison to the Crab spectrum and there are no sharp change in the data points.

Averaged EXO 2030+375 spectrum was well fitted with the model mentioned above. The following results were obtained: power-law spectral index $\alpha = 1.5 \pm 0.2$, $E_{cut} = 37 \pm 4$, $E_{fold} = 32 \pm 4$, $\chi^2_{red} = 1.09$. These spectral parameters are close to those obtained by Reynolds et al. (1993).

6. Conclusions

We present a first INTEGRAL observation of the transient X-ray pulsar EXO 2030+375 with IBIS/ISGRI. We demonstrate that the results on EXO 2030+375 are consistent with those obtained from other X-ray missions. Source light curve shows typical changes in intensity which correspond to the source state in outburst phase. The spectrum of EXO 2030+375 in 20−100 keV energy band is a power-law with a spectral index $\alpha = 1.5$ and has a high energy cutoff above ~30−40 keV.

This letter illustrates the IBIS/ISGRI detector capability to produce scientific results event for partially coded off-axis sources. This capability is one of the most important IBIS/ISGRI characteristics and its exploitation will be very important during the mission.

References

Angelini, L., Stella, L., & Parmar, A. N. 1989, ApJ, 346, 906
Apparao, K. M. V. 1994, Space Sci. Rev., 69, 225
Bazzano, A., Bird, A., Capitanio, F., et al. 2003, A&A, 411, L389
Di Cocco, G., Caroli, E., Celesti, E., et al. 2003, A&A, 411, L189
Goldoni, P., Bonnet-Bidaud, J. M., Falanga, M., et al. 2003, A&A, 411, L399
Goldwurm, A., Pedro, D., Foschini, L., et al. 2003, A&A, 411, L223
Lebrun, F., Leray, J., Lavocate, P., et al. 2003, A&A, 411, L141
Martinez Nuñez, S., Reig, P., Blay, P., et al. 2003, A&A, 411, L411
Parmar, A. N., Stella, L., Ferri, P., & White, N. E. 1985, IAU Circ., 4066
Parmar, A. N., White, N. E., & Stella, L. 1989a, ApJ, 338, 373
Parmar, A. N., White, N. E., Stella, L., Izzo, C., & Ferri, P. 1989b, ApJ, 338, 359
Reig, P., & Coe, M. J. 1999, MNRAS, 302, 700
Quirrenbach, A., Bjorkman, K., Bjorkman, J., et al. 1997, ApJ, 479, 477
Reynolds, A. P., Parmar, A. N., & White, N. E. 1993, ApJ, 414, 302
Ubertini, P., Lebrun, F., Di Cocco, G., et al. 2003, A&A, 411, L131
Wilson, C. A., Finger, M. H., Coe, M. J., et al. 2002, ApJ, 570, 287
Winkler, C., Courvoisier, T., Di Cocco, G., et al. 2003, A&A, 411, L1